IDSA Infectious Diseases Society of America   **hivma** hiv medicine association   OXFORD

Listeria Membrane Protrusion Collapse: Requirement of Cyclophilin A for *Listeria* Cell-to-Cell Spreading

Aaron S. Dhanda,[1] Katarina T. Lulic,[1] A. Wayne Vogl,[2] Margaret M. Mc Gee,[3] Robert H. Chiu,[4,5] and Julian A. Guttman[1]

[1]Department of Biological Sciences, Centre for Cell Biology, Development, and Disease, Simon Fraser University, Burnaby, British Columbia, Canada; [2]Department of Cellular and Physiological Sciences, Faculty of Medicine, University of British Columbia, Vancouver, Canada; [3]School of Biomolecular and Biomedical Science, Conway Institute of Biomolecular and Biomedical Research, University College Dublin, Belfield, Ireland; [4]Dental and Craniofacial Research Institute and School of Dentistry, University of California, Los Angeles; [5]Surgical Oncology and Jonsson Comprehensive Cancer Center, University of California, Los Angeles

Background. *Listeria* generate actin-rich tubular protrusions at the plasma membrane that propel the bacteria into neighboring cells. The precise molecular mechanisms governing the formation of these protrusions remain poorly defined.

Methods. In this study, we demonstrate that the prolyl *cis-trans* isomerase (PPIase) cyclophilin A (CypA) is hijacked by *Listeria* at membrane protrusions used for cell-to-cell spreading.

Results. Cyclophilin A localizes within the F-actin of these structures and is crucial for their proper formation, as cells depleted of CypA have extended actin-rich structures that are misshaped and are collapsed due to changes within the F-actin network. The lack of structural integrity within the *Listeria* membrane protrusions hampers the microbes from spreading from CypA null cells.

Conclusions. Our results demonstrate a crucial role for CypA during *Listeria* infections.

Keywords. cell-to-cell spread; cyclophilin A; *Listeria*; *Listeria monocytogenes*.

Cyclophilin A (CypA) is ubiquitously expressed in all eukaryotic cells as a cytosolic and/or secreted protein [1–3]. As the founding member of a class of enzymes (prolyl *cis-trans* isomerases [PPIases]) that promote protein folding and trafficking through their ability to catalyze the isomerization of peptidyl-prolyl bonds [4], CypA has been reported as an important factor for several biological processes that require actin such as cell migration [3, 5, 6] and general cytoskeletal organization [5].

The actin cytoskeleton is a crucial target of the disease-causing enteric bacterial pathogen, *Listeria monocytogenes*. These bacteria control the host cell's actin polymerization machinery to invade and move within (and amongst) host cells [7]. *Listeria monocytogenes* gain their ability to move within host cells through the actions of the N-WASp mimicking bacterial surface protein ActA, which hijacks and activates the Arp2/3 complex at the bacterial surface in order to generate branched actin-rich comet tails that propel the bacteria forwards [8]. Movement of the bacteria amongst cells relies on the generation of modified comet tails that form membrane protrusions when the bacteria engage the plasma membrane at the border of the host cells [7]. These actin-rich protrusions cause corresponding invaginations in the neighboring cells, which ultimately enable *L monocytogenes* to be disseminated from one cell to another.

In this study, we demonstrate that *L monocytogenes* hijack CypA exclusively at their actin-rich membrane protrusions. Using cells depleted of CypA, we show that these protrusions are structurally collapsed due to the actin network within the structures being morphologically altered at the bacterial attachment site. This results in a significant decrease in the ability of *L monocytogenes* to spread from cell to cell. *Listeria monocytogenes* infections of the null cells that are complemented with green fluorescent protein (GFP)-CypA reverts the phenotype of the collapsed protrusions to being indistinguishable from those generated in wild-type (WT) cells. Collectively, our findings highlight a novel actin-associated role of a cellular PPIase during the proper formation and function of actin-rich structures that are essential for the progression of *L monocytogenes* infections.

METHODS

Cell Culture

Human cervical (HeLa) and human lung (A549) epithelial cells were acquired from American Type Culture Collection (catalog numbers CCL-2 and CCL-185). Cyclophilin A WT (*PPIA*^{+/+}) and CypA knockout ([KO] *PPIA*^{−/−}) mouse embryonic fibroblast cells (MEFs) were generated previously [9]. HeLa cells, CypA WT MEFs, and CypA KO MEFs were cultured using Dulbecco's modified Eagle's medium (DMEM) containing high glucose (Hyclone, GE Healthcare) supplemented with 10% fetal bovine serum (FBS) (Gibco, Thermo Fisher Scientific). SKOV3 cells were cultured using DMEM: nutrient mixture F-12 (DMEM/F-12; Gibco, Thermo Fisher Scientific) supplemented with 10% FBS. A549 cells were cultured using Ham's F-12K (Kaighns's) medium (Gibco, Thermo Fisher Scientific)

supplemented with 10% FBS. All cell lines were maintained in a cell culture incubator (37°C, 5% CO_2). To seed cells for experiments, flasks with cells were washed 3 times with Dulbecco's phosphate-buffered saline (PBS) without Ca^{2+} and Mg^{2+} (PBS [−/−]) (Gibco, Thermo Fisher Scientific), trypsinized with 0.05% Trypsin-EDTA (Gibco, Thermo Fisher Scientific), and then seeded onto clear polystyrene 6-well format plates (Corning) containing glass coverslips. For electron microscopy experiments, flexible silicone elastomer membranes (Flexcell International) were used in place of glass coverslips.

Bacterial Strains and Growth Conditions

The bacterial strains used were *L monocytogenes* strains EGD BUG 600 and Δ*actA* (gifted by Dr Pascale Cossart). All strains were grown at 37°C in brain heart infusion (BHI) agar or broth (BD Biosciences).

Listeria monocytogenes Infections

To infect cultured cells, overnight shaken broth cultures of *L monocytogenes* were diluted 10× in BHI broth and then incubated at 37°C in a shaking incubator until $A_{600} = 1.00$. Once cultures reached $A_{600} = 1.00$, bacteria were spun down for 5 minutes at 10 000 rpm (25°C) and washed with PBS [−/−]. Pelleted bacteria were resuspended with serum-free media then diluted 100×. Diluted bacteria were added onto culture plates containing host cells and incubated for 30 minutes to study bacterial internalization for at least 6 hours, to study comet tails and actin-rich protrusion formation.

Reagents and Antibodies

Antibodies and reagents used in this study included the following: Alexa Fluor 594-, 488-, and 350-conjugated phalloidin (Invitrogen); Alexa Fluor 594-, 488-, and 350-conjugated goat anti-rabbit and goat anti-mouse antibodies (2 μg/mL; Invitrogen); rabbit anti-CypA A (10 μg/mL for immunofluorescence and 1 μg/mL for Western blot [ab41684; Abcam]); mouse anti-ezrin (1:100 for immunofluorescence [CPTC-Ezrin-1; Developmental Studies Hybridoma Bank]); mouse anti-N-WASP (4 μg/mL for immunofluorescence [sc-100964; Santa Cruz Biotechnology]); mouse anti-α tubulin (1:1000 for Western blot [12G10; Developmental Studies Hybridoma Bank]); rabbit anti-*L monocytogenes* (1:300 for immunofluorescence [223021; BD Difco]); horseradish peroxidase-conjugated goat anti-rabbit and goat anti-mouse antibodies (1 μg/mL; Invitrogen); CellTracker Blue (Invitrogen); Neutral Red (72210; Sigma-Aldrich) CypA (working concentration of 20 μM; Abcam); and LIVE/DEAD Viability/Cytotoxicity Kit, for mammalian cells (Thermo Fisher Scientific). The mouse monoclonal anti-α-tubulin antibody (12G10) was deposited to the Developmental Studies Hybridoma Bank (DSHB) by Frankel, J./Nelsen, E.M. (University of Iowa). The mouse monoclonal anti-ezrin antibody (CPTC-Ezrin-1) was deposited to the DSHB by Clinical Proteomics Technologies for Cancer.

Deoxyribonucleic Acid Constructs

Deoxyribonucleic acid plasmids encoding GFP-CypA and GFP-CypA-R55A were generated previously [5, 10].

Microscopy

Images were acquired using a Leica DMI4000B (Leica Microsystems) inverted fluorescent microscope fitted with a Hamamatsu Orca R2 CCD camera (Hamamatsu Photonics). All devices were controlled by MetaMorph Imaging System software (Universal Imaging). Images obtained were evaluated using Metamorph Imaging System software or ImageJ.

Immunolocalization

Fixation and immunolocalization procedures can be found in Supplemental Methods.

Cell-to-Cell Spreading Assay

Cell-to-cell spreading assay procedures can be found in Supplemental Methods.

Plaque Assay

Plaque assay procedures can be found in Supplemental Methods.

Gentamicin Protection Assay

Gentamicin protection assay procedures can be found in Supplemental Methods.

Cell Culture Transfections

Cell culture transfection procedures can be found in Supplemental Methods.

Cyclophilin A Ribonucleic Acid Interference Knockdown

Ribonucleic acid (RNA) interference procedures can be found in Supplemental Methods.

Lysate Preparation and Western Blotting

Preparation of lysates and Western blotting methods can be found in Supplemental Methods.

Electron Microscopy

Electron Microscopy techniques can be found in Supplemental Methods.

Statistical Analysis

Statistical analysis overview can be found in Supplemental Methods.

RESULTS

Cyclophilin A Is Recruited Exclusively to *Listeria monocytogenes* Actin-Rich Membrane Protrusions

Listeria monocytogenes harness the actin polymerization machinery of their host cells at 4 distinct times in their infectious cycle: (1) during host cell invasion, (2) at actin-rich clouds surrounding stationary bacteria, (3) at comet tails used for intracellular actin-based motility, and (4) when spreading from one cell to

another using actin-rich membrane protrusions. To investigate whether CypA was recruited to any of these bacterially generated actin-rich sites, we infected HeLa cells with WT *L monocytogenes* and stained fixed cells using anti-CypA antibodies. We found that CypA was present at *L monocytogenes*-generated membrane protrusions but was absent from all other actin-rich sites during these infections (Figure 1A). Cyclophilin A stabilizes N-WASp through its GPXLP motif [5], implying that CypA could be involved in actin regulation. Because *L monocytogenes* uses an N-WASp mimic that does not contain the GPXLP site, this suggested to us that the observed CypA recruitment to the actin protrusions was independent of N-WASp. To confirm this, we costained infected cells with anti-CypA and anti-N-WASp antibodies. As expected, N-WASp was absent from the *L monocytogenes* protrusions (Figure 1C). The altered localization of CypA in infected cells did not correspond to a change in expression levels when compared with uninfected cells (Figure 1D). We also performed infections using an *L monocytogenes actA*-deletion mutant, which is unable to generate F-actin networks at its surface, and found that CypA was not present at the surface of these bacteria (Supplementary Figure 1).

To further validate our findings, we transfected GFP-CypA into HeLa cells and assessed its presence at *L monocytogenes* membrane protrusions when expressed in a protrusion originating cell (sending cell) or a protrusion engulfing cell (receiving cell). The GFP-CypA was present only at membrane protrusions originating from a sending cell but not at *L monocytogenes* membrane protrusions or protrusion invaginations when expressed in receiving cells (Figure 1B).

Cyclophilin A Is Required for the Proper Formation of *Listeria monocytogenes* Membrane Protrusions

To determine the functional importance of CypA at *L monocytogenes* membrane protrusions, we infected cells depleted of CypA (CypA KO) with *L monocytogenes* and saw that they were severely misshapen when compared with their counterparts in CypA WT cells (Figure 2A and B). Those structures (confirmed using the *L monocytogenes* membrane protrusion marker, ezrin) did not stretch outwards from the host cell and appeared collapsed (Figure 2C). To confirm that collapsed *L monocytogenes* protrusions were not a cell-line specific phenotype, we preformed small interfering RNA (siRNA)-mediated knockdowns of CypA in the A549, SKOV3, and HeLa cell lines. As expected, CypA was enriched at *L monocytogenes* protrusions in cells treated with control nontargeting siRNA (Supplementary Figure 2A), whereas in cell lines with CypA knocked down, we saw similar collapsed protrusions (Supplementary Figure 2B) as noted in the CypA KO cells (Figure 2). A potential reason for the collapsed protrusions could be the generation of an unfavorable intracellular environment over the course of infection due to high bacterial loads. To test this, we examined *L monocytogenes* protrusions generated in CypA KO cells infected with

fewer than 10 bacterial cells. We saw that, even in cells with low infection levels, *L monocytogenes* protrusions were still collapsed (Supplementary Figure 3).

To gain further insight into the collapsed *L monocytogenes* membrane protrusions, we used transmission electron microscopy. *Listeria monocytogenes* membrane protrusions are generally straight in their appearance and contain proximally located branched F-actin that broadens into a relatively uniform thickness at the base of the bacteria (Figure 2D, left). We found that the overall appearance of collapsed protrusions in CypA KO cells was dramatically altered at the ultrastructural level. We noticed that the actin did not originate as a broad band at the base of some protrusions, but rather it came from a narrow zone, which then flared into a broad array more distally (Figure 2D, middle). Other protrusions showed a misorientation of actin filaments along the lateral side of the microbes and a lack of uniformity within the structures (Figure 2D, right).

When CypA KO cells were transfected with either GFP-CypA or an enzymatic mutant (GFP-CypA-R55A), the WT morphology of the *L monocytogenes* protrusions was rescued (Figure 2E), suggesting that the PPIase activity of CypA is likely dispensable at *L monocytogenes* protrusions. Furthermore, we saw no alteration to the protrusions in CypA WT cells that were transfected with GFP-CypA-R55A compared with cells transfected with GFP-CypA (Supplementary Figure 4).

Because CypA is a protein that is also secreted from cells [2], we investigated whether secreted CypA could play a role in *L monocytogenes* actin-rich protrusion formation. We initially probed the supernatants of cultured CypA WT cells and found that CypA is in fact secreted from the WT cells (Supplementary Figure 5A). To ascertain the role of secreted CypA on *L monocytogenes* protrusion formation, we added 24-hour spent media from cultured CypA WT and CypA KO cells as well as fresh culture media separately onto infected CypA KO cells. In all cases, the *L monocytogenes* protrusions remained collapsed, suggesting that intracellular CypA is the functioning source of the protein at the structures (Supplementary Figure 5B).

Cyclophilin A PPIase activity is a well known target of the immunosuppressive drug cyclosporin A (CsA). To test whether treatment of cells with CsA would affect *L monocytogenes* protrusion formation, we treated infected CypA WT cells with CsA (20 μM) and examined *L monocytogenes* membrane protrusions. Similar to our results using GFP-CypA-R55A, inhibition of CypA PPIase activity did not alter CypA recruitment to the *L monocytogenes* protrusions (Supplementary Figure 6). Because CypA was not present at comet tails, it was not surprising that they remained morphologically indistinguishable between the KO and WT CypA cells (Supplementary Figure 7A and B). Taken together, these data indicate that CypA is needed for proper *L monocytogenes* membrane protrusion formation as well as F-actin organization within the structures and does so independently of its PPIase activity.
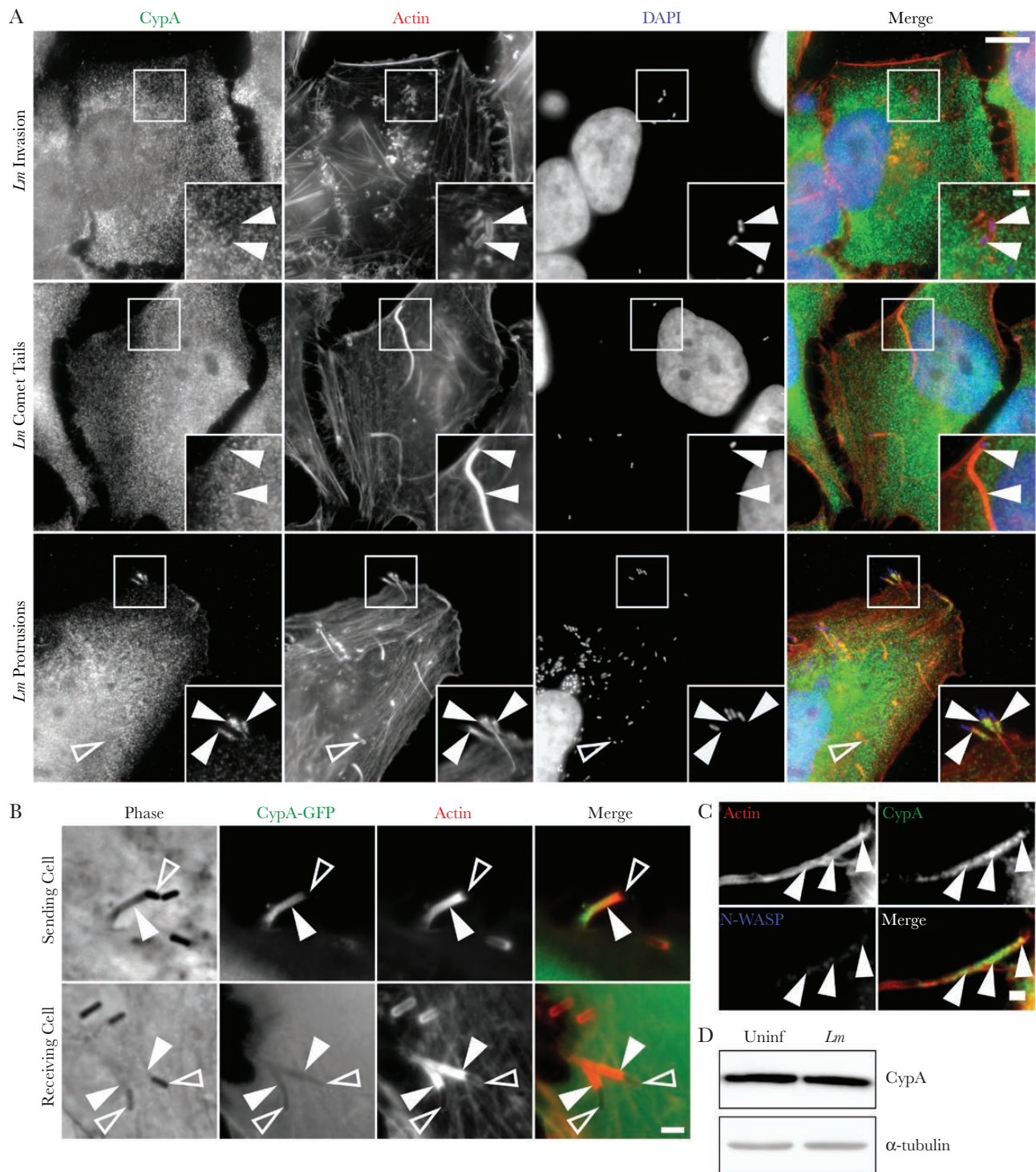
Figure 1. Cyclophilin A (CypA) is recruited to *Listeria monocytogenes* (*Lm*)-containing membrane protrusions. (A) HeLa cells infected with wild-type *Lm* for 30 minutes (invasion) or 6 hours (comet tail and protrusion formation) were fixed then stained with a rabbit polyclonal CypA targeting antibody (green), Alexa594-phalloidin (red) to visualize F-actin, and 4',6-diamidino-2-phenylindole ([DAPI] blue) to visualize deoxyribonucleic. Cyclophilin A is recruited to protrusions but no other bacterially generated actin-rich structures. Solid arrowheads within insets (enlargement of boxed regions) indicate, from top to bottom, bacterial invasion sites, a comet tail, and multiple protrusions. Absence of CypA at actin clouds is indicated by open arrowheads. Scale bars are 10 μm and 2 μm (insets). (B) HeLa cells expressing green fluorescent protein (GFP)-CypA were infected with *L monocytogenes*. Green fluorescent protein-CypA is present at *L monocytogenes* protrusions moving from GFP-CypA-positive HeLa cells (Sending Cell) into GFP-negative cells, but not at protrusions or protrusion invaginations when GFP-CypA is expressed in a receiving cell (Receiving Cell). Open arrowheads indicate bacteria, and solid arrowheads point to *L monocytogenes* protrusions and invaginations. Scale bar is 2 μm. (C) Protrusion from a HeLa cell infected with *L monocytogenes* showing CypA enrichment and N-WASp absence at the structure. Actin is shown to identify the *L monocytogenes* protrusion (arrowheads). Scale bar is 1 μm. (D) Western blot of uninfected (left) and 8-hour *L monocytogenes* infected (right) HeLa whole-cell lysate probed with a rabbit polyclonal CypA targeting antibody shows no alteration in CypA protein levels. The blot was stripped and reprobed with a mouse anti-α tubulin antibody to confirm equal loading.
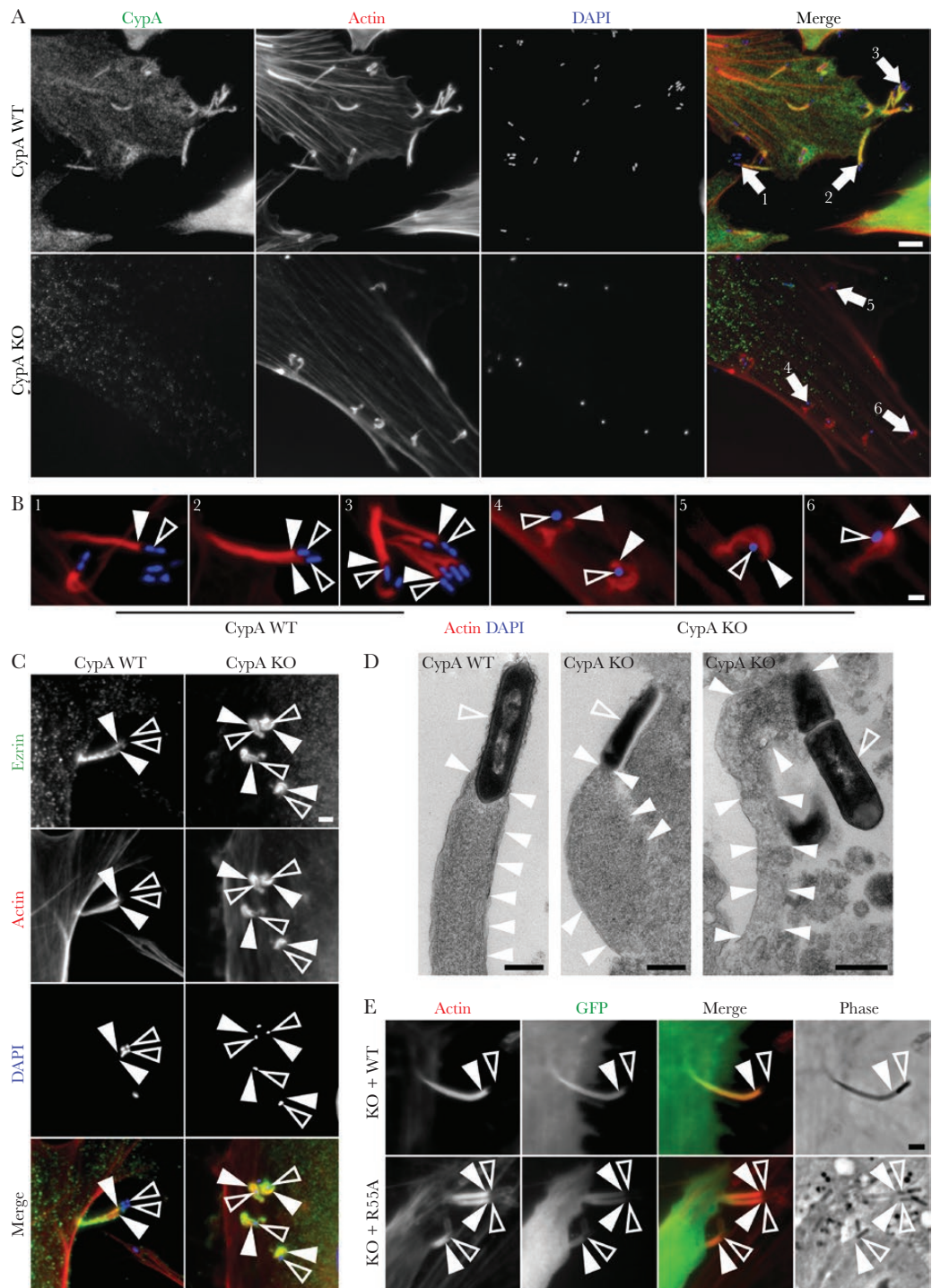
---

4 • **JID 2018:XX (XX XXXX)** • Dhanda et al

Figure 2. Cyclophilin A (CypA) is crucial for proper F-actin organization and attachment within *Listeria monocytogenes* membrane protrusions. (A) CypA wild-type (WT) and CypA knockout (KO) cells infected with *L monocytogenes* (blue) were fixed then stained using a rabbit polyclonal CypA targeting antibody (green). Cyclophilin A is abundant at normal actin-rich (red) *L monocytogenes* protrusions (arrows) extending outwards from host CypA WT cells (top). *Listeria monocytogenes* protrusions (arrows) in CypA KO cells (bottom) are collapsed and highly twisted. Scale bar is 5 μm. (B) Enlargement of *L monocytogenes* protrusions labeled in (A). Open arrowheads indicate *L monocytogenes* bacteria (blue), whereas solid arrowheads point to the corresponding protrusions (red). Color intensities were enhanced from (A) to clearly identify the bacteria and protrusions. Scale bar is 1 μm. (C) Ezrin immunolocalization (green) at actin-rich *L monocytogenes* membrane protrusions (red) generated in CypA WT and CypA KO cells. Ezrin is present at WT and collapsed *L monocytogenes* protrusions. Open arrowheads indicate the location of *L monocytogenes* bacteria (blue), whereas solid arrowheads point to the protrusions. Scale bar is 1 μm. (D) Transmission electron micrographs of morphologically normal *L monocytogenes* membrane protrusions generated in CypA WT cells (left) and protrusions from CypA KO cells (middle and right). Open arrowheads indicate bacteria, whereas solid arrowheads point to protrusions. Scale bars are 500 nm. (E) Cyclophilin A KO cells were rescued by transfection of green fluorescent protein (GFP)-CypA (top) or the enzymatic mutant GFP-CypA-R55A (bottom). *Listeria monocytogenes* protrusions in those cells appear morphologically normal in the presence of either GFP-CypA or GFP-CypA-R55A. Open arrowheads indicate *L monocytogenes* (phase contrast), whereas solid arrowheads point to the rescued protrusions. Scale bar is 2 μm.

Cyclophilin A Is Important for *Listeria monocytogenes* Cell-to-Cell Spreading

Our observations of collapsed *L monocytogenes* protrusions in cells depleted of CypA suggested that the projection of the structures into neighboring cells and thus the cell-to cell transfer of bacteria might be affected. We initially quantified the abundance of the *L monocytogenes* protrusions compared with all actin-rich structures (clouds, comet tails, and protrusions) formed by *L monocytogenes* in CypA null cells compared with CypA WT cells. We found that CypA expression increased the amount of protrusions per infected cell (Supplementary Figure 8A). To test the importance of CypA for *L monocytogenes* cell-to-cell spreading, we modified a mixed-cell population cell-to-cell spreading assay [11]. This allowed us to quantify the number of *L monocytogenes* protrusions moving from unlabeled protrusion-sending cells (either CypA WT or CypA KO) into uninfected, but labeled (CellTracker Blue), *L monocytogenes* protrusion-receiving cells (CypA WT) (Figure 3A). As expected, most protrusions originating from CypA KO cells were collapsed (Figure 3A and Supplementary Figure 8B). However, we were able to detect a few protrusions moving from one cell to another (Figure 3A and Supplementary Figure 8C). We calculated a ~2.5-fold increase in the number of protrusions moving cell-to-cell when they were generated in cells expressing CypA (Figure 3B). We also noticed that protrusions moving from CypA WT cells formed clusters of multiple protrusions, whereas CypA KO cells projected only single bacteria whose protrusions were extremely thin (Figure 3A and Supplementary Figure 8C). We also tested whether using CypA KO cells as the protrusion-receiving cell in the spreading assays would alter the efficiency of bacterial cell-to-cell transfer. In these assays, we detected similar collapsed protrusion phenotypes as well as a ~3-fold spreading deficit from bacteria in CypA KO protrusion-sending cells (Figure 3C and D).

We next performed plaque assays, another commonly used method to further assess bacterial spreading as well as cytotoxicity resulting from *L monocytogenes* infections. We were surprised to find that plaques were generated in monolayers of CypA KO cells infected with *L monocytogenes* after only 48 hours (Supplementary Figure 9A and B). In contrast, no plaques could be identified at the same time point in infected monolayers of CypA WT cells (Supplementary Figure 9A and B). We examined host cell viability earlier in the infections to try to tease out a potential explanation behind the plaque assays. We found that samples of infected CypA KO cells formed numerous clusters of dying cells compared with infected WT samples, which showed only spaced out and individual dying cells (Supplementary Figure 9C). Because of this, we thought one likely scenario to explain the early appearance of plaques could occur from elevated bacterial loads in CypA KO cells compared with WT cells, resulting in more rapid and aggressive cytotoxicity. We performed gentamicin protection assays to enumerate the number

of intracellular bacteria during infections and found a 3-fold increase in the number of intracellular bacteria within CypA KO cells compared with WT cells (Supplementary Figure 10A). We also saw abundant clustering of bacteria in CypA KO cells compared with WT cells during early infection time points (Supplementary Figure 10B). Taken together, these findings reveal that although CypA functions normally to restrict bacterial invasion, it is hijacked later by *L monocytogenes* to promote the efficient cell-to-cell spreading of the bacteria.

DISCUSSION

In this study, we demonstrate a unique role for CypA in stabilizing actin-rich membrane protrusions generated by *L monocytogenes* and thus facilitating *L monocytogenes* infection by directly promoting the association of protruding bacteria with neighboring host cells during bacterial spreading events. In addition, our findings reveal a novel actin-associated role for CypA that does not depend on N-WASp.

Cyclophilin A directly interacts with and stabilizes N-WASp, a cellular activator of Arp2/3-based F-actin nucleation/polymerization [5]. However, the actin-based propulsion and spreading of *L monocytogenes* relies solely on the bacterial surface N-WASp-mimicking protein, ActA, to activate the Arp2/3 complex, because *L monocytogenes* bacteria readily generate motile comet tails in vitro when coincubated with purified actin polymerization components that do not include N-WASp [8, 12]. Although ActA is a very efficient N-WASp mimic, it is not identical, and a number of our findings strongly suggest that CypA may associate with alternative sites at actin-rich structures. First, we find CypA enriched throughout the networked actin-rich core of the *L monocytogenes* protrusions rather than just at the bacterial surface where ActA is present. Second, CypA is known to require the GPXLP motif within N-WASp [5], which is absent in ActA. Third, CypA is completely absent from cytosolic actin-rich comet tails. This final point suggests that accessory proteins present at protrusions but not at comet tails might be key for CypA association at those structures. Our finding that the actin network originates from alternative (narrow or lateral) regions on the bacteria suggests that this host protein may influence the localization of ActA on *L monocytogenes*. This would be the first evidence of a host protein altering the positioning of a bacterial cell surface effector and will require more investigation. Recent studies have uncovered that the secreted *L monocytogenes* protein InlC promotes bacterial spreading via its ability to perturb apical junction integrity through antagonism of the host adaptor Tuba [13]. Tuba and its binding partners N-WASp, Sec31, and Sec13 normally restrict bacterial spreading by generating tension at the cell borders [13, 14]. Whereas here we show that CypA within the actin-core of protrusions promotes efficient bacterial cell-to-cell spreading, whether or not CypA at apical junction complexes
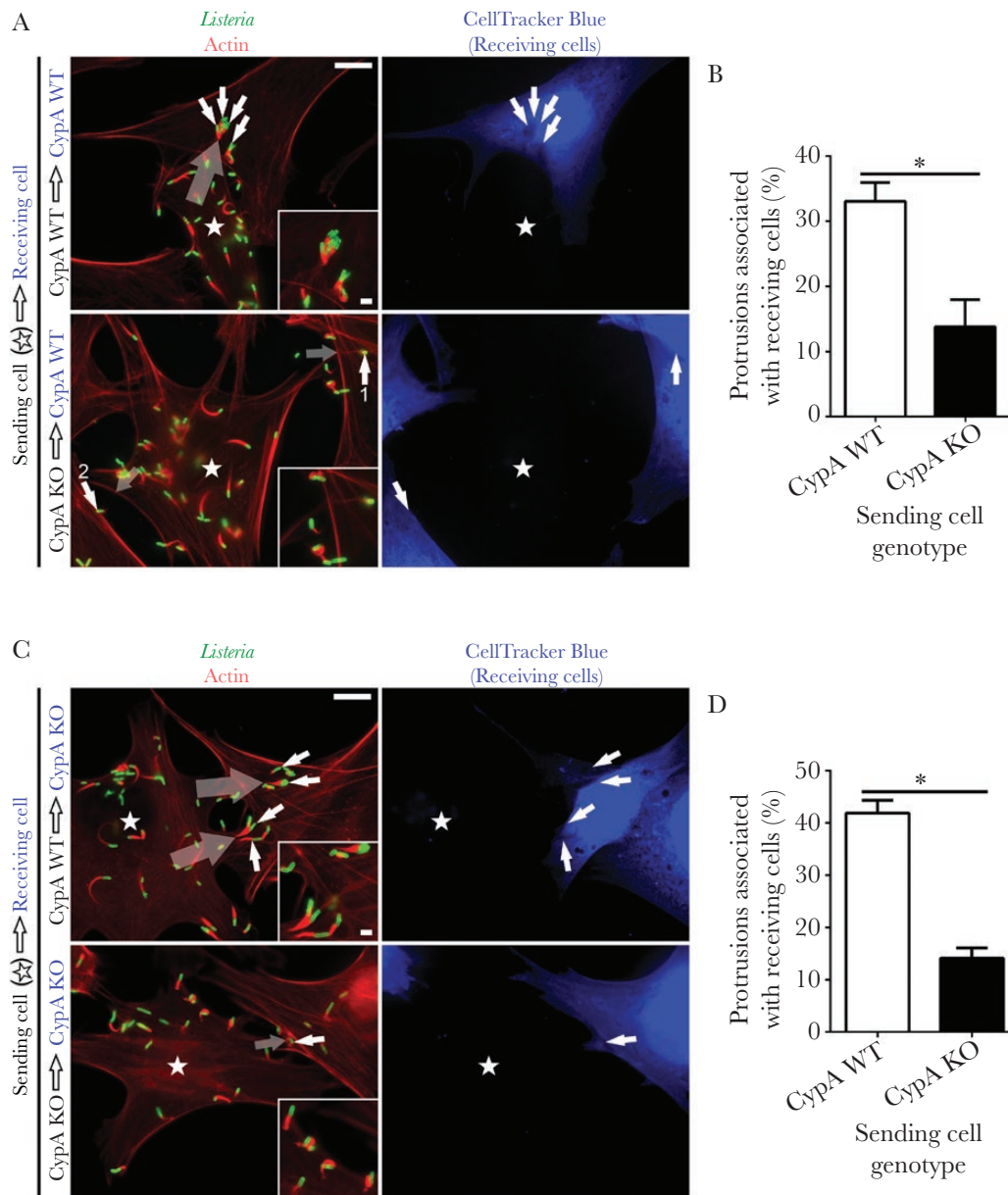
Figure 3. Cyclophilin A (CypA) promotes *Listeria monocytogenes* cell-to-cell spreading. (A) Micrographs representative of cell-to-cell spread assays. Cyclophilin A wild-type ([WT] top) or CypA knockout ([KO] bottom) cells infected with *L monocytogenes* were overlaid onto cultures of uninfected CypA WT cells (blue cells). Stars indicate the cell that is sending the *L monocytogenes* membrane protrusions (white arrows) that are moving into uninfected CypA WT cells (blue). Translucent arrows indicate the direction of bacterial dissemination. Fewer and thinner protrusions (numbered arrows; see also Supplemental Figure 7C) move from CypA KO cells into neighboring cells. *Listeria monocytogenes* bacteria are immunolabeled using a rabbit anti-*L monocytogenes* antibody (green), and F-actin is stained using Alexa594-phalloidin (red). Insets are enlargements of actively spreading bacteria. Scale bars are 10 μm and 2 μm (insets). (B) Proportion of *L monocytogenes* membrane protrusions moving from CypA WT or CypA KO cells into neighboring CypA WT receiving cells. Data are presented as a bar graph of the average value ± standard error of the mean (s.e.m.) from 3 independent experiments (24 infected cells counted for each sending cell genotype). The average percentage of protrusions associated with neighboring CellTracker-labeled cells is as follows: 32.9% (from CypA WT sending cells) and 13.8% (from CypA KO sending cells). (C) Micrographs representative of cell-to-cell spread assays. Cyclophilin A WT (top) or CypA KO (bottom) cells infected with *L monocytogenes* were overlaid onto cultures of uninfected CypA KO cells (blue cells). Stars indicate the cell that is sending the *L monocytogenes* membrane protrusions (white arrows) that are moving into uninfected CypA KO cells (blue). Translucent arrows indicate the direction of bacterial dissemination. Fewer and thinner protrusions move from CypA KO cells into neighboring cells. *Listeria monocytogenes* bacteria are immunolabeled using a rabbit anti-*L monocytogenes* antibody (green), and F-actin is stained using Alexa594-phalloidin (red). Insets are enlargements of actively spreading bacteria. Scale bars are 10 μm and 2 μm (insets). (D) Proportion of *L monocytogenes* membrane protrusions moving from CypA WT or CypA KO cells into neighboring CypA KO receiving cells. Data are presented as a bar graph of the average value ± s.e.m. from 3 independent experiments (24 infected cells counted for each sending cell genotype). The average percentage of protrusions associated with neighboring CellTracker-labeled cells is as follows: 41.9% (from CypA WT sending cells) and 14.1% (from CypA KO sending cells).

augments junctional tension through N-WASp or is hijacked by the bacteria for their spread will require further study.

The most dramatic effects we saw were the collapse of actin-rich membrane protrusions in cells depleted of CypA. This is a rarely seen phenotype that has only been observed with inhibition of the ezrin/radixin/moesin (ERM) family protein ezrin, a well known cytoskeletal-plasma membrane linker [15]. Unlike ezrin, we suspect that CypA does not directly interact with and stabilize actin filaments within the growing *L monocytogenes* protrusions, because this protein does not possess any known actin-binding motifs. One possibility to explain this stabilizing role is that CypA within the structures is used in a complex to properly recruit or activate other F-actin stabilizers such as ezrin within the *L monocytogenes* protrusions. Because ezrin (and other ERM proteins) is known to require activation via phosphorylation to interact with actin filaments and stabilize these structures, this may explain our finding of altered F-actin networks and collapsed protrusions in the CypA null cells [15, 16].

CONCLUSIONS

In conclusion, we have shown that CypA is an integral factor for the proper formation of *L monocytogenes* actin-rich membrane protrusions and that cell-to-cell spreading of *L monocytogenes* is significantly attenuated in the absence of CypA. The novel role this molecular chaperone plays at these bacterially generated structures could have broad applications to other membrane/actin-rich sites within the cell as well as other pathogens that co-opt the host actin cytoskeleton for their disease progression.

Supplementary Data

Supplementary materials are available at *The Journal of Infectious Diseases* online. Consisting of data provided by the authors to benefit the reader, the posted materials are not copyedited and are the sole responsibility of the authors, so questions or comments should be addressed to the corresponding author.

Notes

References

1. Ryffel B, Woerly G, Greiner B, Haendler B, Mihatsch MJ, Foxwell BM. Distribution of the cyclosporine binding protein cyclophilin in human tissues. Immunology **1991**; 72:399–404.

2. Sherry B, Yarlett N, Strupp A, Cerami A. Identification of cyclophilin as a proinflammatory secretory product of lipopolysaccharide-activated macrophages. Proc Natl Acad Sci U S A **1992**; 89:3511–5.

3. Xu Q, Leiva MC, Fischkoff SA, Handschumacher RE, Lyttle CR. Leukocyte chemotactic activity of cyclophilin. J Biol Chem **1992**; 267:11968–71.

4. Lang K, Schmid FX, Fischer G. Catalysis of protein folding by prolyl isomerase. Nature **1987**; 329:268–70.

5. Calhoun CC, Lu YC, Song J, Chiu R. Knockdown endogenous CypA with siRNA in U2OS cells results in disruption of F-actin structure and alters tumor phenotype. Mol Cell Biochem **2009**; 320:35–43.

6. Saleh T, Jankowski W, Sriram G, et al. Cyclophilin A promotes cell migration via the Abl-Crk signaling pathway. Nat Chem Biol **2016**; 12:117–23.

7. Tilney LG, Portnoy DA. Actin filaments and the growth, movement, and spread of the intracellular bacterial parasite, *Listeria monocytogenes*. J Cell Biol **1989**; 109:1597–608.

8. Welch MD, Iwamatsu A, Mitchison TJ. Actin polymerization is induced by Arp2/3 protein complex at the surface of *Listeria monocytogenes*. Nature **1997**; 385:265–9.

9. Sun S, Guo M, Zhang JB, Ha A, Yokoyama KK, Chiu RH. Cyclophilin A (CypA) interacts with NF-κB subunit, p65/RelA, and contributes to NF-κB activation signaling. PLoS One **2014**; 9:e96211.

10. Bannon JH, O'Donovan DS, Kennelly SM, Mc Gee MM. The peptidyl prolyl isomerase cyclophilin A localizes at the centrosome and the midbody and is required for cytokinesis. Cell Cycle **2012**; 11:1340–53.

11. Czuczman MA, Fattouh R, van Rijn JM, et al. *Listeria monocytogenes* exploits efferocytosis to promote cell-to-cell spread. Nature **2014**; 509:230–4.

12. Loisel TP, Boujemaa R, Pantaloni D, Carlier MF. Reconstitution of actin-based motility of *Listeria* and *Shigella* using pure proteins. Nature **1999**; 401:613–6.

13. Rajabian T, Gavicherla B, Heisig M, et al. The bacterial virulence factor InlC perturbs apical cell junctions and promotes cell-to-cell spread of *Listeria*. Nat Cell Biol **2009**; 11:1212–8.

14. Gianfelice A, Le PH, Rigano LA, et al. Host endoplasmic reticulum COPII proteins control cell-to-cell spread of the bacterial pathogen *Listeria monocytogenes*. Cell Microbiol **2015**; 17:876–92.

15. Pust S, Morrison H, Wehland J, Sechi AS, Herrlich P. *Listeria monocytogenes* exploits ERM protein functions to efficiently spread from cell to cell. EMBO J **2005**; 24:1287–300.

16. Nakamura F, Huang L, Pestonjamasp K, Luna EJ, Furthmayr H. Regulation of F-actin binding to platelet moesin in vitro by both phosphorylation of threonine 558 and polyphosphatidylinositides. Mol Biol Cell **1999**; 10:2669–85.